Dust Collection Efficiency for Power Law Bodies in Hypersonic Flight

JOSEPH H. SPURK* AND NATHAN GERBER†
Ballistic Research Laboratories, U.S. Army Aberdeen Research and Development Center, Aberdeen Proving Ground, Md.

A numerical and analytical study predicts 1) the collection efficiency of conical and blunted axisymmetric bodies of the power law family in hypersonic flight through dust clouds and 2) the impact angle and velocity. Collection efficiencies of cones using the exact conical flowfield solutions are shown for particles obeying a drag law of the form $C_D = fn(Re, M, T_p/T)$. Most of the data can be correlated by three dimensionless groups. Results show large variations from collection efficiency based on the less realistic "standard" drag law $C_D = fn(Re)$. Collection efficiency of power law bodies has been determined in the hypersonic slender body approximation for the realistic drag law. The data correlate well with the three aforementioned dimensionless parameter groups. Blunting is found to decrease collection efficiency appreciably. An approximate model provides a qualitative description of the collection efficiency and impact angle dependence on the main parameters. The distribution of impact angle for cones and blunt bodies also correlates well with the three dimensionless groups. In all cases, the impact velocity is nearly equal to the flight velocity.

Nomenclature

a = speed of sound, m/sec
c = specific heat of dust particle $[m^2/(sec^2\,°K)]$ ($\cong 850$)
c_b, c_s = constants in body and shock shapes, respectively; i.e., $r_b = c_b t^k$, $r_s = c_s t^k (c_b/c_s = \lambda_b)$
c_p, c_v = specific heats of gas at constant pressure and volume, respectively, $m^2/(sec^2\,°K)$
C_D = dust particle drag coefficient, based on area $= \pi\sigma_p^2$
E = collection efficiency (ratio of number of particles hitting the body to the number that would hit body if undeflected)
f = $(9/2)\mu L/(\rho_p \sigma_p^2 U_\infty \varepsilon)$—dimensionless parameter group
f_b = $(9/2)\mu_s r_{pb}/(\rho_p \sigma_p^2 U_\infty r_{pb}/\chi_{pb})$
g = $12.12\,\sigma_p \rho_p/(L\rho_\infty)$—dimensionless parameter group
g_b = $12.12\,\sigma_p \rho_p/(r_{pb}\rho_\infty)$
h = heat-transfer coefficient, $kg/(sec^3\,°K)$
k = exponent in power law body ($r \sim x^k$)
$\mathcal{K}$ = coefficient of heat conduction, $kg\,m/(sec^3\,°K)$
ℓ = length of body, m
L = radius of body base, m
M = particle Mach number relative to gas
M_∞ = flight Mach number of body
Nu = $2h\sigma_p/\mathcal{K}$—Nusselt number
p = gas pressure, $kg/(m\,sec^2)$
Pr = $\mu c_p/\mathcal{K}$—Prandtl number
q = speed of particle relative to gas, m/sec
r = radial coordinate, m
r_b = radial coordinate of point on body, m
r_{pb} = value of r where particle strikes body, m
r_{ps} = value of r where particle enters shock layer, m
R_{gas} = gas constant, $m^2/(sec^2\,°K)$, (=288.02 for air)
Re = $2\rho q\sigma_p/\mu$—Reynolds number
t = time, sec
T, T_p = gas and particle temperatures, respectively, °K
u, u_p = axial component of gas and particle velocities, respectively, m/sec
$\vec{u}, \vec{u}_p$ = vector representation of gas and particle velocities, respectively
U_∞ = speed of body through gas, m/sec
v, v_p = radial component of gas and particle velocities, respectively, m/sec
v_s = shock wave velocity in approximate model, m/sec
v_p^* = particle speed after traversing outer zone in approximate model, m/sec
x = axial coordinate, m
γ = c_p/c_v—ratio of specific heats of gas (=1.4 for air)
ε = L/ℓ—thickness ratio of body
θ = spherical polar coordinate (longitudinal angle)
θ_b = cone half-angle
θ_{im} = impact angle (angle between tangent to body and particle trajectory)
θ_{sl} = $\tan^{-1}(dr_b/dx_b)$ at point of impact
λ = self-similar flow independent variable
λ_b = λ evaluated on body
μ = viscosity coefficient, kg/(m sec)
$\mu = \mu_0 (T/T_0)^{3/2}(T_0+110)(T+110)^{-1}$
$(T_0 = 293.2,\ \mu_0 = 17.96 \times 10^{-6})$
ρ, ρ_∞ = gas density and freestream gas density, respectively, kg/m^3
ρ_p = particle material density, kg/m^3
σ_p = radius of spherical particle, m
τ = particle relaxation time [definition following Eq. (9)]

Subscripts
b = body
p = dust particle
pb = body at location of particle impact
s = shock wave
∞ = freestream
0 = reference condition

Received October 14, 1971; revision received January 21, 1972. The authors wish to express their appreciation to B. Bilsborough, who programed the calculations for the BRLESC.

Index categories: Multiphase Flows; Supersonic and Hypersonic Flow.

* Supervisory Aerospace Engineer. Associate Fellow AIAA.
† Aerospace Engineer. Member AIAA.

I. Introduction

THE flow of gas containing small solid or liquid particles around a body is of considerable interest in various technical applications. In such two-phase flows the gas phase flowfield will in general differ from the corresponding field in pure gas because energy and momentum are withdrawn from the gas phase. (In general, it is assumed that the particle also can contribute to the momentum.) Since the exchange processes require a certain time for completion, relaxation effects occur. On the other hand, the solid particle trajectories are of course also different in the flowfield environment than, say, in vacuum or in a uniform stream.

The number of particles actually hitting the body and their size and physical parameters are important if one wishes to estimate the erosion damage to a vehicle or if one wishes to know the distribution of particles collected by a vehicle flying through dust

clouds. If the mass ratio of the particulate phase to the gas phase is small enough, then the coupling from the solid phase to the gaseous phase may be neglected, i.e., the particle phase does not affect the gas phase. Particle interaction also can be neglected if the volume ratio is low enough, this however being a more restrictive assumption. The problem then reduces to computation of the particle trajectories in a given flowfield.

The flowfields considered here are hypersonic slender body flowfields; more specifically hypersonic fields around power law bodies. Using the equivalence principle one may formulate the hypersonic steady flow problems in terms of known solutions to unsteady one dimensional problems. As is well known, the applicability of these solutions (except for the cone) requires the freestream pressure to be very small or the freestream Mach number be very large. The basic assumptions then for the flowfield are $\theta_b \ll 1$; $M_\infty \gg 1$. For the cone neither of these assumptions is necessary for self-similar flow and the cone will serve as test case to evaluate the effect that the hypersonic small disturbance assumptions have on the collection efficiency.

Recently, two publications appeared which have similar objectives. Probstein and Fassio[1] compute the collection efficiency for hypersonic constant density flows around wedges, cones and spheres under the assumption that the particle Mach number is very small. The standard drag curve is used and, to provide convenient expressions for integration of particle equations, is divided in three regions: 1) low Reynolds number region where Stokes' law is applicable 2) an intermediate region and 3) a high Reynolds number region where the drag coefficient is independent of Reynolds number, i.e., where the drag is considered purely inertial. It is further assumed that the particle during the whole trajectory stays within one of the three regions. The computations are done for slender wedges and cones $\theta_b \ll 1$, i.e., for conditions where the hypersonic small disturbance theory is also applicable. The results of Ref. 1 can therefore be compared with our computations. In particular, the unrealistic assumption of incompressible drag curve can be evaluated and also the effect of assuming only one drag law for the whole trajectory.

Wüst in Ref. 2 has computed the collection efficiency for continuum and free molecular flow for wedges and for plates, the latter aligned normal to the flow. Again, for the continuum flow the particle is assumed to obey one drag law only during the whole trajectory; explicit expressions are found for the linear drag law (Stokes' law) and the quadratic drag law (inertial law) for the limiting case that the particle Mach number is very small. Numerical results are given for the efficiency in the free molecular flow regime. Wüst's data cannot be compared with the present data which applies only to axisymmetric bodies. However since no hypersonic nor slender body approximation is actually made in Ref. 2, the data can be used to evaluate the approximation of Ref. 1.

II. Drag Law

The drag coefficient or "drag curve" used in the present computations is the drag curve applicable to a perfectly smooth sphere in a uniform steady flow of a perfect gas. Thus, effects on the drag resulting from the velocity and pressure gradient and temperature gradient in the actual shock layer are neglected. Compared to the inertia term in the equation of motion, these terms are small of order ρ/ρ_p for the velocity and temperature effects[11] and, in the case considered here, also for the pressure gradient term, consistent with the assumption made already that the flow is unaffected by the presence of the solid particle; then the pressure gradient term $\partial p/\partial x$ may be replaced by $\rho\, Du/Dt$.

Taking into account effects of inertia, viscosity, compressibility and heat conduction, dimensional analysis[3] shows that the drag coefficient may be expressed as

$$C_D = fn(Re, M, Pr, T_p/T_0, C/T_0, \gamma)$$

The ratio of specific heats $c_p/c_v \equiv \gamma$ and the Prandtl number $Pr \equiv \mu c_p/\kappa$ depend on the structure of the gas and are usually not explicitly listed since most experiments are conducted using air. The parameter C/T_0 enters through the specific assumption of Sutherland's formula for variation of viscosity and coefficient of heat conduction with temperature. This parameter is absent if the viscosity is assumed to be proportional to the temperature. The parameter T_p/T_0 is also due to effects of heat transfer. Experiments show that the effect of heat transfer on the drag coefficient is quite small except in the free molecular and the slip flow regime. In the continuum flow regime the drag coefficient is only a function of Reynolds number and Mach number under the assumption made above and under the restriction that the flow media have the same values of γ and Pr. For incompressible flow $M \to 0$, C_D depends only on the Reynolds number, and the relation $C_D = fn(Re)$ is referred to as the standard drag curve and used often in two phase flow computation even under circumstances where compressibility effects must be expected. The analytical prediction of the drag coefficient has been only possible in the case of free molecular flow and in the continuum flow regime under conditions where the inertia and compressibility effects are small. Basically the flow in the wake of a sphere is unsteady and this is a serious hindrance in the analysis. Numerical integration of the Navier-Stokes equations even in the compressible case has become possible but is restricted to rather low Reynolds number and steady wake flow situations. The numerical computations still present many serious problems, and one should not expect reliable drag information over a wide Reynolds number range in the near future. Practically all of today's information on the drag curve is thus empirical with the incompressible case the most thoroughly investigated.

Various empirical relations have been formulated to represent the drag coefficient C_D as functions of Mach number and Reynolds number. One of the better known formulations is due to Carlson and Hoglund.[4] Crowe[5] has devised another expression which removes some objections against Carlson's formulations. Crowe's expression gives approximately the correct limiting behavior as the molecular flow regime is approached, where it also accounts for heat-transfer effect. The expression is formulated to give the experimental value of C_D at $M = 2$ and $M = 0$ for Reynolds number $< 5 \times 10^3$. The largest possible particle Mach number in our case is equal to the Mach number formed with the disturbance velocity right behind the shock. This Mach number cannot be larger than 1.89 ($\gamma = 1.4$); thus it would appear that Crowe's formulation is best suited for our computations. Recent measurement by Zarin[6] show that Crowe's empirical relation predicts the drag coefficient very well in the subsonic slip flow regime. For supersonic flow Crowe showed that his formula evaluated for $M = 3$ predicts the drag coefficient well up to a Reynolds number of 10^3. The relation is of the form

$$C_D = fn(M, Re, T_p/T_0)$$

and explicitly given by

$$C_D = (C_{D\,\mathrm{inc}} - 2)\exp\left[-(3.07\gamma^{1/2}(M/Re)_{\not\kappa}(Re)\right] + (\not\kappa/\gamma^{1/2}M)\exp(-Re/2M) + 2 \qquad (1)$$

$$\log_{10}{}_{\not\kappa} = 1.25\left[1 + \tanh(0.77\log_{10}Re - 1.92)\right]$$

$$\not\kappa = 2.3 + 1.7(T_p/T)^{1/2} - 2.3\tanh(1.17\log_{10}M)$$

For $M \to 0$ the standard drag curve $C_D = C_{D\,\mathrm{inc}}$ is produced.

Under the assumptions made the motion of the spherical particle is described by

$$d\vec{u}_p/dt = 3/8\,(\rho/\rho_p)(C_D/\sigma_p)|\vec{u} - \vec{u}_p|(\vec{u} - \vec{u}_p) \qquad (2)$$

In order to evaluate C_D according to (1) in the low Re regime the particle temperature must be known. The temperature relaxation is described by the energy equation of the particle

$$dT_p/dt = (3h/\rho_p c\sigma_p)(T - T_p) \qquad (3)$$

where the heat-transfer coefficient is expressed in terms of the Nusselt number

$$Nu = 2h\sigma_p/\not\kappa \qquad (4)$$

Kavanau[7] has related the Nusselt number in the slip flow regime to the value the Nusselt number would have if there was no temperature jump by the relation

$$Nu = Nu^{(0)}/\{1+3.42[M/(Pr\,Re)]Nu^{(0)}\} \quad (4a)$$

Here $Nu^{(0)}$ is the Nusselt number without temperature jump. Carlson and Hoglund have chosen for $Nu^{(0)}$ the empirical expression for incompressible steady continuum flow

$$Nu_c = 2+0.459\,Re^{0.55}\,Pr^{0.33} \quad (5)$$

With this choice Nu tends to Nu_c for large Re and, for $Pr = 1$, Nu approaches the free molecular flow values predicted by Sauer. Crowe's expression for the drag, together with the above expression for the heat transfer coefficient, is used as basis for our trajectory computation. The relation has been used for Reynolds number $<10^4$, but in the vast majority of computed cases the particle Reynolds number is well below 10^3. It is well to keep in mind that these expressions are empirical and are extrapolated here in Mach number and Reynolds number regions where little or no experimental data exist.

III. Cone

The supersonic flowfield around a cone is self-similar without the restriction resulting from the hypersonic small disturbance assumption. The equations describing the flowfield may be found in standard textbooks on gas dynamics.[8] In the numerical integration it is convenient to treat the inverse problem, i.e., to compute, for a given conical shock front, the flow until the body is reached. If U, V, W are the velocity components in a spherical polar coordinate system R, θ, ϕ then the body is reached when $V = 0$. It is therefore convenient to consider V as an independent variable. Taking the cylindrical symmetry and the self-similar property into account the equations describing the inviscid perfect gas flow around a cone are given by

$$d\theta/dV = -[U+(U+V\cot\theta)/(1-V^2/a^2)]^{-1};\quad dU/dV = V(d\theta/dV)$$
$$dp/dV = -\rho V[1+U(d\theta/dV)];\quad dT/dV = (R_{\text{gas}}\,T/pc_p)\,dp/dV;$$
$$p = \rho R_{\text{gas}}\,T \quad (6)$$

The particle path is referred to a cylindrical coordinate system r, x with the velocity components v, u (see Fig. 1). The equations of motion in the r and x direction for the particle are respectively

$$dv_p/dV = [(v-v_p)\tau^{-1}](d\theta/dV)(d\theta/dt)^{-1}$$
$$du_p/dV = [(u-u_p)\tau^{-1}](d\theta/dV)(d\theta/dt)^{-1} \quad (7)$$

Here $d\theta/dt$ is taken along the solid particle path and given by

$$d\theta/dt = x_p^{-1}\cos^2\theta(v_p-u_p\tan\theta) \quad (8)$$

The velocity components in the cylindrical coordinate system are related to U, V by

$$u = (U^2+V^2)^{1/2}\cos(\theta+\tan^{-1}V/U)$$
$$v = (U^2+V^2)^{1/2}\sin(\theta+\tan^{-1}V/U) \quad (9)$$

The relaxation time τ is

$$\tau = [\tfrac{3}{8}C_D(\rho/\rho_p)(q/\sigma_p)]^{-1}$$

where $q = [(u-u_p)^2+(v-v_p)^2]^{1/2}$ is the magnitude of the relative velocity between gas phase and the solid particle. The particle trajectory is found from

$$dx_p/dV = u_p(d\theta/dV)(d\theta/dt)^{-1}$$
$$dr_p/dV = v_p(d\theta/dV)(d\theta/dt)^{-1} \quad (10)$$

The collection efficiency (the ratio of number of particles hitting the body to the number that would hit the body if undeflected) is then given by

$$E = (r_{ps}/r_{pb})^2 \quad (11)$$

IV. Power Law Bodies

Among the class of one-dimensional unsteady, self-similar flows are the motions produced by a cylindrically expanding piston where the piston velocity is proportional to some power of time. Similarity solutions exist when 1) the initial pressure is zero or 2) the piston velocity is constant. According to Hayes' equivalence principle the solution to these unsteady one dimensional problems can be immediately adapted to axisymmetric hypersonic flow over slender bodies, and represent bodies with power law shapes ($r_b \sim x^k$) in hypersonic flow. The case $k = 1$ represents the flow over a cone and does not require $p_\infty = 0$. In order to have non-negative slopes on the body, the exponent is restricted by $\frac{1}{2} < k$. For $k > 1$ the bodies are cusped and concave. Thus practical hypersonic shapes are obtained for $\frac{1}{2} < k \leqq 1$.

The ordinary differential equations describing the self-similar flow and the boundary conditions appropriate to self-similarity have been formulated by a number of authors. We will use the equations and boundary conditions in the form and notation given in Hayes and Probstein[9]; their representation is essentially the same as that of Sedov.[3] Reference 9 may also be consulted for an account of the historical development of the subject.

The independent similarity variable of Ref. 9 is defined by the relation

$$\lambda = Br\,t^{-k}$$

and the dependent variables by

$$V = vr^{-1}t;\quad R = \rho\rho_\infty^{-1};\quad P = p(\rho_\infty r^2 t^{-2})^{-1}$$

If these definitions are substituted into the equations of motion of one-dimensional unsteady compressible flow, there results

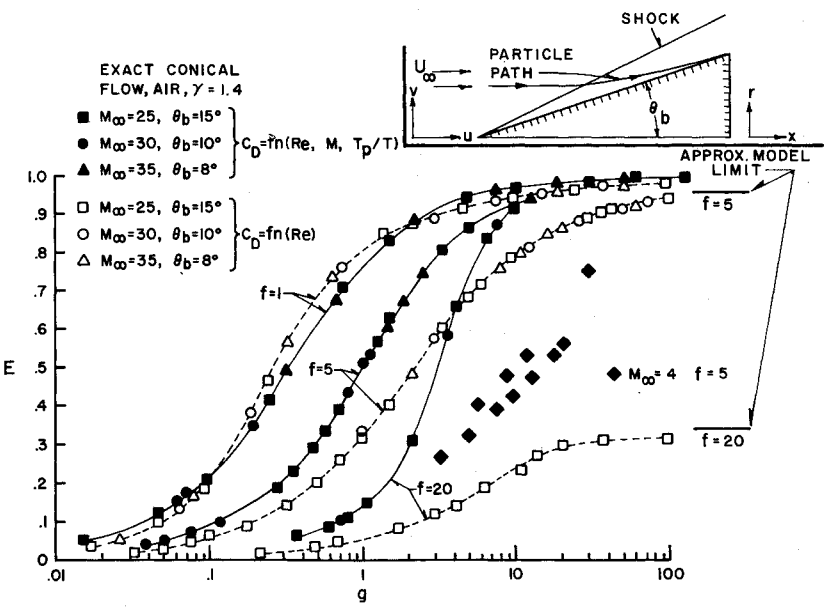

Fig. 1 Collection efficiency for conical body—correlation of data with g and f, comparison of standard and general drag law effects.

three coupled ordinary equations for P, R, V, viz. Eqs. (2.6.5) of Ref. 9:

$$\lambda[(V-k)(dV/d\lambda)+R^{-1}(dP/d\lambda)] = -V(V-1)-2PR^{-1}$$
$$\lambda[(dV/d\lambda)+(V-k)R^{-1}(dR/d\lambda)] = -2V$$
$$\lambda(V-k)[P^{-1}(dP/d\lambda)-\gamma R^{-1}(dR/d\lambda)] = -2(V-1)$$

This set of equations, as shown by Sedov,[3] may be reduced to one ordinary differential equation [(2.6.7) of Ref. 9] for z as a function of V, where $z = \gamma PR^{-1}$.

For the numerical integration the above equations are solved for the derivatives $dV/d\lambda$, $dR/d\lambda$, $dP/d\lambda$, and then integrated by the Kutta-Merson algorithm, using the variables right behind the shock [Eq. (2.6.12) of Ref. 9] as initial conditions

$$V_s = 2k/(\gamma+1), \quad R_s = (\gamma+1)/(\gamma-1), \quad P_s = 2k^2/(\gamma+1)$$

Since the body is a singular point of the system of equations, an approximate solution near $V = k$ is patched to the numerical solution and given by

$$\lambda = c_1(V-\delta)^{-1/2}; \quad (\delta = [1-k]/\gamma)$$
$$P = c_2; \quad R = c_3(V-k)^{\delta/(k-\delta)}$$

The constants c_i, $i = 1,2,3$, are determined from the last numerically obtained point.

The equations of the dust particle in the transverse plane are

$$dv_p/d\lambda = (v-v_p)\tau^{-1}\,dt/d\lambda \tag{12a}$$

and

$$dr_p/d\lambda = v_p\,dt/d\lambda \tag{12b}$$

where $dt/d\lambda$ is taken along the particle path

$$dt/d\lambda = \lambda^{-1}[(v_p/r_p)-(k/t)]^{-1} \tag{13}$$

In the axial direction the disturbance velocity is small of second order in ε so that the particle position in x is

$$x_p = U_\infty t + \text{const}$$

The constant is the value of the abscissa at which the particle enters the shock. The collection efficiency is again given by Eq. (11). The collection efficiency can thus be completely determined in the unsteady equivalent problem of an expanding cylinder. In this picture the collection efficiency is the ratio of particles caught by the expanding cylinder to the number of particles the cylinder would encounter if there were no disturbance produced in the medium ahead of the cylinder.

V. An Approximate Model

The exact solutions of the one-dimensional motions produced by point explosions or expanding pistons show that the phenomena of interest occur in a thin layer near the shock (or body for $k > 1$). This fact has prompted the use of integral methods, especially by Chernyi,[10] in analogy with the use of integral methods in boundary-layer theory. The integral methods have been applied to the unsteady or hypersonic problems (via the equivalence principle) in various degrees of sophistication. A review of these methods may be found in Ref. 9.

Basic to the integral method is of course the assumption on the distribution of flow variables across the layer, the simplest assumption being that the variables are constant. For the purpose of obtaining a simple model for the dependence of the collection efficiency on the relevant parameters one divides the shock layer in two regions: 1) a region immediately behind the shock, of thickness Δ, which contains almost all the mass between shock and body; and 2) a layer between the body and the previous layer which contains just enough mass to allow a finite pressure, so that the kinetic energy is negligible in this region but not the internal energy.

From conservation of mass, momentum, and energy in integral form, and with the assumption of constant velocity equal to velocity right behind the shock, (or to the same approximation equal to the shock velocity itself), one obtains for a piston expanding according to the power law the following relation for the pressure:

$$p = \alpha p_s \qquad (\alpha = [3k-1]/2k) \tag{14}$$

and for the ratio of shock to body radius

$$(r_s/r_b)^2 = (\gamma+1)(3k-1)[(\gamma+1)k-1]/(2k-1)[(5\gamma+1)k-(\gamma+1)] \tag{15}$$

This result is given by Chernyi[10] as an example of the application of integral methods. Though the division of the shock layer into two zones is not necessary for this result, this concept leads to a simple expression for collection efficiency.

In the limit the thickness of the layer $\Delta \to 0$ and the particle Reynolds number $\to \infty$, so that the drag in the outer zone is purely inertial ($C_D = \text{const}$). After the particle leaves this layer, the drag may be either completely neglected or may be based on the low Reynolds number law.

For the equation of motion in the high-density layer one has

$$dv_p/dt = \tfrac{3}{8}(C_D/\sigma_p)(\rho/\rho_p)[v(t)-v_p]^2 \tag{16}$$

where $v(t) = [2/(\gamma+1)]v_s(t)$. This equation can be reduced to a Riccati equation for $v_s \sim t^{k-1}$ and integrated to give $v_p(t)$ in terms of Bessel functions of order k^{-1}. However, a much simpler result is obtained if $v(t)$ during the very short transit time across the layer is considered constant. Then (16) may be written

$$\frac{8\sigma_p\rho_p}{(3C_D)}\int_0^{v_p^*} v_p(v-v_p)^{-2}\,dv_p = \int_{r_s}^{r_s+\Delta}\rho\,dr \tag{17}$$

The right-hand side is equal to $\rho\Delta$ and, using conservation of mass, may be replaced by $(\frac{1}{2})(\rho_\infty r_s)$. Integrating the expression on the left side and rearranging leads to

$$(v_p^*/v)[1-(v_p^*/v)]^{-1}+\log_e[1-(v_p^*/v)] = E^{1/2}g^{-1} \tag{18}$$

where

$$g = 12.12\rho_p\sigma_p/(L\rho_\infty)$$

with $C_D = 0.44$ and $E = (r_{ps}/r_{pb})^2$, since r_s is obviously equal to r_{ps}, the radius at which the shock reaches the particle; r_{pb} is the radius at which the piston reaches the particle and corresponds to the base radius L of the body in the hypersonic equivalence.

For negligible drag in the inner layer r_{pb} follows from

$$r_{pb} = r_{ps}+v_p^*(t_{pb}-t_{ps}) \tag{19}$$

where t_{pb} and t_{ps} are the times at which the piston and shock wave, respectively, reach the particle. Since $r_s = c_s t^k$ say, and $r_b = c_b t^k$, it follows that

$$E^{-1/2} = \frac{r_{pb}}{r_{ps}} = 1+\frac{v_p^*}{r_{ps}}\left[\left(\frac{r_{pb}}{c_b}\right)^{1/k}-\left(\frac{r_{ps}}{c_s}\right)^{1/k}\right] \tag{20}$$

This equation may be rearranged to give

$$\frac{v_p^*}{v} = \frac{\gamma+1}{2k}\frac{(1-E^{1/2})E^{(1-k)/(2k)}}{[(c_s/c_b)^{1/k}-E^{1/(2k)}]} \tag{21}$$

where $c_s/c_b = r_s/r_b$ is given by Eq. (15). Equation (21) and Eq. (18) give an implicit relation of the form $E = fn(g)$; hence, according to the simplified model, the collection efficiency depends only on the dimensionless group $(\rho_p/\rho_\infty)(\sigma_p/L)$. Such a relation holds exactly also for power law bodies with constant drag coefficient.

The drag in the inner layer, assuming a Stokes drag law, can conveniently be accounted for only in the case of the cone, i.e., $k = 1$. Even then the viscosity can be fixed only by an ad hoc assumption. It may be shown that for the cone in order to account for the drag in the inner layer Eq. (21) should be replaced by

$$[2(\gamma+1)^{-1}(r_s/r_b)](v_p^*/v) = 1-E^{1/2}f[1-(r_b/r_s)]\cdot$$
$$[1-\exp\{-f+fE^{1/2}(r_b/r_s)\}]^{-1} \tag{22}$$

This equation follows from the integration of the particle equation of motion in the inner layer after some manipulation in complete analogy to Eqs. (19, 20, and 21). Here a new dimensionless group

$$f = (9/2)\mu L/(\rho_p\sigma_p^2 U_\infty\varepsilon)$$

appears which accounts for the viscous drag. It will be shown later that f (with μ evaluated behind the shock at the point at which the particle enters the shock) and g correlate all of the numerical data quite well.

The approximate model can also be employed to determine

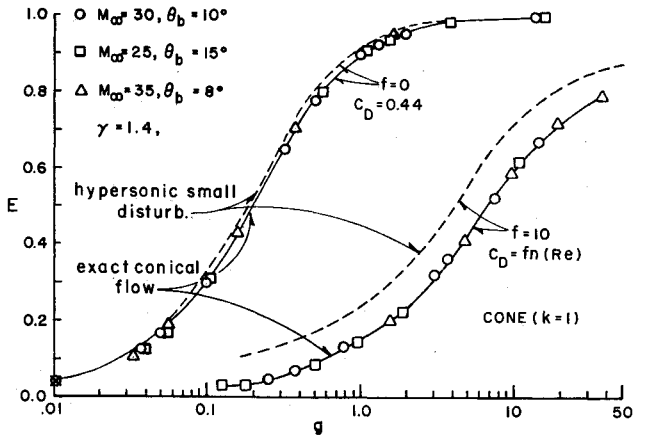

Fig. 2 Collection efficiency for conical body—comparison of hypersonic small disturbance theory results with exact conical flow results.

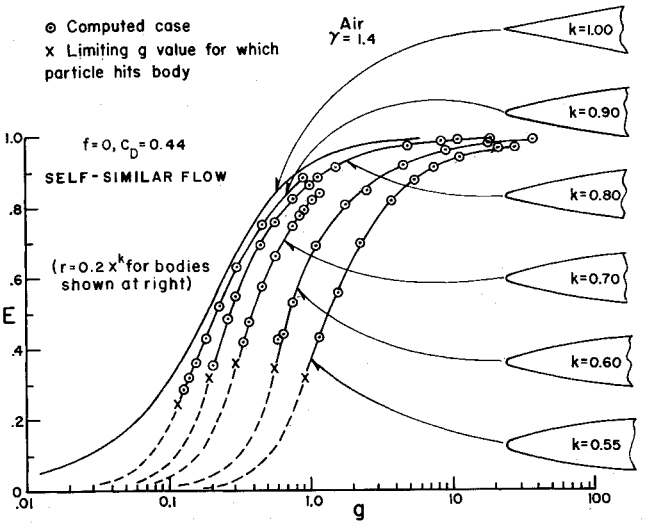

Fig. 4 Collection efficiency for power law bodies—$C_D = 0.44$, hypersonic small disturbance theory.

the dependence of the angle of impact θ_{im} on the problem parameters and the body radius at the location of impact. Accordingly, where θ_{sl} is the slope angle of the body at the impact point,

$$\theta_{im}/\theta_{sl} = 1 - [\tan^{-1}(v_p^*/U_\infty)/\tan^{-1}(dr/dx)_{pb}]$$

By Eqs. (18, 21, and 22) this expression simplifies for small values of body slope to

$$\theta_{im}/(\theta_{sl}) = fn(g_b, f_b) \tag{23}$$

The index b indicates that L in the dimensionless groups f and g has been replaced by the body radius at the impact point. This relation also correlates very well all the numerical data.

VI. Discussion of Results

Figure 1 shows the collection efficiency for a conical body, based on the exact conical flowfield, as a function of g and f. The solid points give the efficiency for the general drag law $C_D = fn(R_e, M, T_p/T)$, the open symbols the efficiency for the standard drag law. The differences in E for larger values of f are very pronounced where the curves for $C_D = fn(Re)$ tend to limiting values different from 1 as $g \to \infty$. The limiting value for $g \to \infty$ is recovered in the simple model discussed in Sec. V and is indicated on the graph. Despite the large effect the particle Mach number has on these results (as the comparison of solid and open symbols show) the data are well correlated by the two groups g and f, although neither contains the Mach number explicitly. For the hypersonic flows considered in these computations, the Mach number behind the shock and, in fact, in the shock layer is the same for all cases so that the particles experience a similar "Mach number history."

For supersonic Mach number the correlation is expected to fail, and this is indicated by points shown on the graph which are computed for a free stream Mach number of 4 and different cone angles. The effect on the drag of heat transfer to the particle becomes important only in the near free molecular flow, and for the cases considered is apparently not important enough to affect the correlation.

Figure 2 compares the collection efficiency computed on the basis of the hypersonic small disturbance theory with collection efficiency based on the exact conical flowfield computation. For $f = 0$ and for the large Mach numbers the difference between the two curves is very small, expectedly so; however for larger viscous effects, the difference is larger, as the two curves computed for $f = 10$ indicate.

In Fig. 3 the efficiency is plotted versus β_i, which is the parameter chosen by Probstein and Fassio.[1] As mentioned earlier, these authors assume that the particle during the whole trajectory stays within one of the three regimes into which the standard drag curve was divided. The index i denotes the regime used in their computations; and β_i changes with i, so that the abscissa is different for different regimes. Computations were based on exact conical flow, using the fit of Ref. [ ] to the standard drag curve; however, the appropriate drag region was used according to the actual particle Reynolds number. The parameter used in plotting

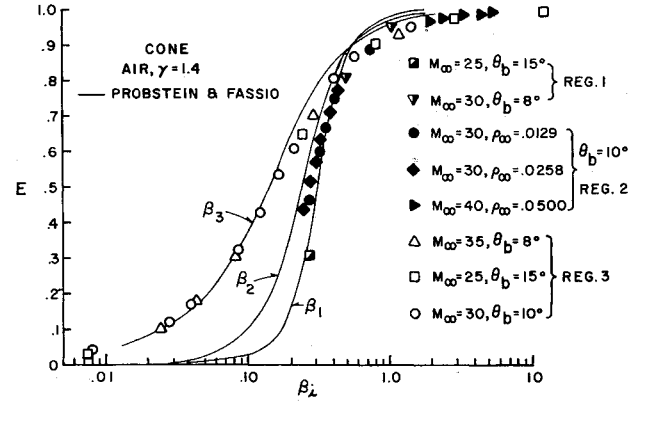

Fig. 3 Collection efficiency for conical body—comparison of Ref. 1 results with exact conical flow computations using standard drag law.

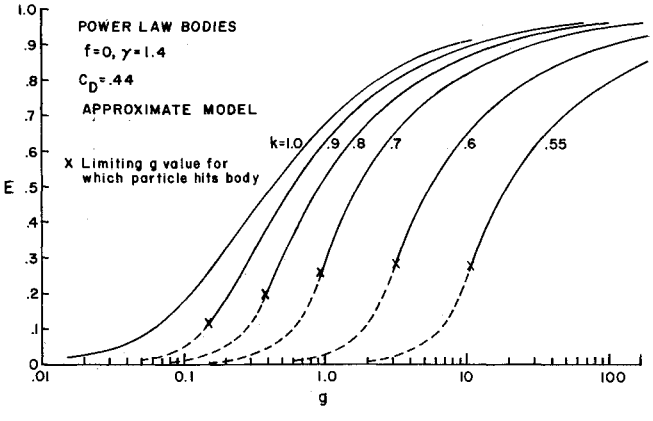

Fig. 5 Collection efficiency for power law bodies—$C_D = 0.44$, approximate model.

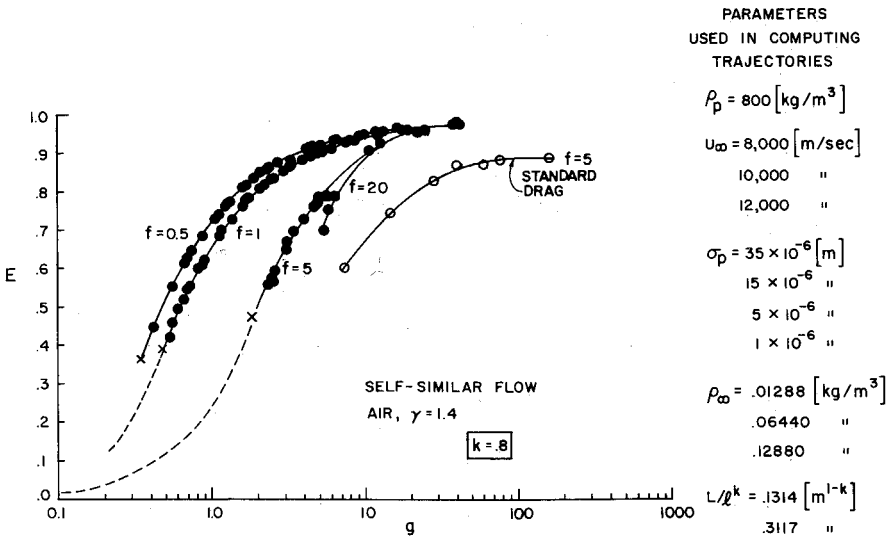

Fig. 6 Collection efficiency for power law bodies—$k = 0.8$, general drag law, hypersonic small disturbance theory.

the results in this figure is the parameter corresponding to the drag regime in which the particle finds itself right behind the shock.

The results of Ref. 1 are in good agreement with the exact computation; this agreement lends support to the use of only one regime in the entire particle trajectory computation. This, in effect, amounts to extrapolating the chosen drag regime beyond its range of applicability. However, a comparison of the three regime fit to the standard drag curve (Fig. 1 of Ref. 1) shows that such an extrapolation, even over considerable Re range, will not substantially affect the drag coefficient.

Figure 4 shows the collection efficiency based on the similarity solution for power law bodies for $f = 0$. The efficiency is seen to be a function only of g, and specifically independent of U_∞ and the thickness ratio ε. For $f = 0$ this is to be expected since the collection efficiency is completely determined by the behavior of the variables in the equivalent unsteady problem and the velocity and length scales enter the hypersonic steady flow problem then only through the transformation $t = xU_\infty^{-1}$. The graph clearly shows the significant reduction in the collection efficiency that is due to blunting. For $k < 1$ there is a value of g below which the number of particles hitting the body will not increase even if the body base diameter is increased. In the unsteady picture this corresponds to the case where the dust particles have been accelerated to a velocity large enough that the piston in the later (slower) stages of its motion cannot catch up with them. In the equivalent steady picture this corresponds to the case where the particles have been deviated by the blunt nose so that the slope of their trajectory is larger than the body slope. Beyond the limiting g value the efficiency E is proportional to g^2 and the function $E = E_{\lim} g_{\lim}^{-2} g^2$ is shown in the graph. This limiting point can only be found approximately in the numerical computation. However this behavior is shown by the approximate model also, where the limiting point can be found analytically. The collection efficiency for the approximate model is shown in Fig. 5; and it is seen that this model predicts the qualitative behavior of E quite well, though it is not usable for quantitative predictions.

Figure 6 shows the collection efficiency for the general drag law for $k = 0.8$ and various values of f (with μ evaluated on the trajectory right behind the shock). The correlation of the data in terms of f and g is quite good, again for the same reason as for the cone. Behind the shock the particle Mach number is equal to the Mach number of the disturbance velocity, which is the same for all cases. Nevertheless compressibility effects are large, as the inspection of the curves based on the standard drag law shows. Figure 7 shows the efficiency for the general drag law for $k = 0.9$, and it seems that the correlation with g and f is similarly good. A careful comparison of Figs. 6 and 7 shows that the beneficial effect of blunting noticed from Fig. 4 is enhanced when a realistic drag law is used.

Since f is an implicit function of E through the value of the

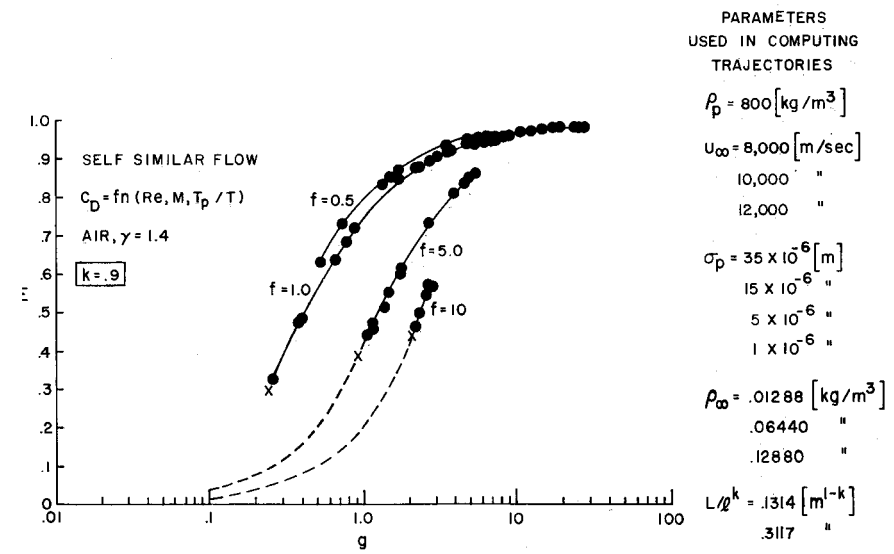

Fig. 7 Collection efficiency for power law bodies—$k = 0.9$, general drag law, hypersonic small disturbance theory.

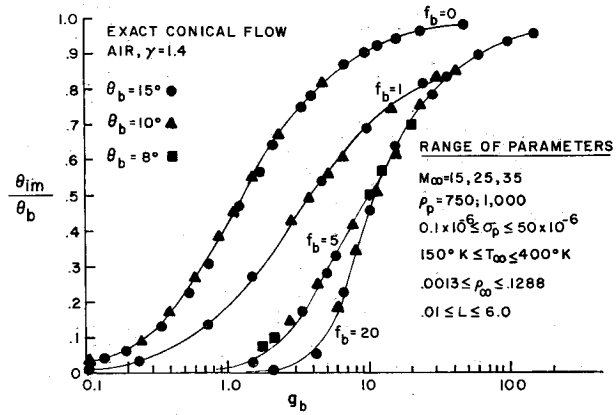

Fig. 8 Impact angle of particle on conical body—correlation of data with g_b and f_b.

viscosity behind the shock at r_s, it is necessary to use a successive approximation procedure to determine E for a given body, using Fig. 6 (or 7). For example one may use an approximate value for f, then determine an approximate E, and thus, r_s and a new approximation for f.

The results of the computation for power law bodies are of course afflicted by the local failure of the equivalence principle near the nose. This failure manifests itself in the "entropy layer"

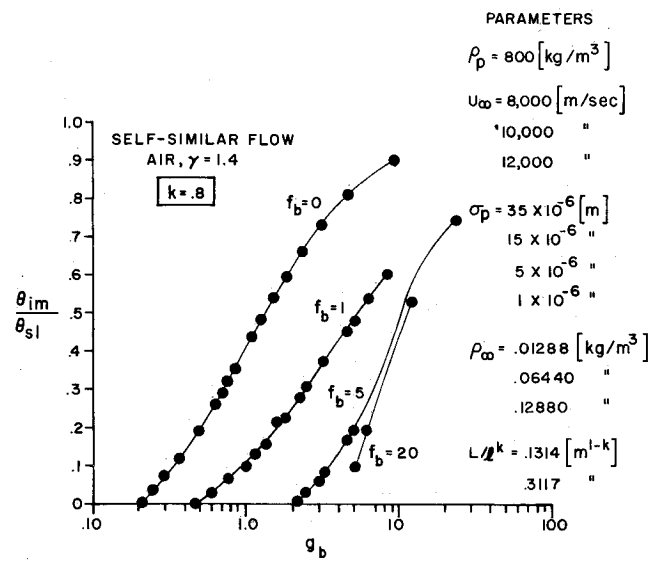

Fig. 9 Impact angle of particle on power law body, $k = 0.8$—correlation of data with g_b and f_b.

of Ref. 9. For $k > 0.65$ for our case the effect of the entropy layer on the flowfield is negligible according to a criterion by Sychev.[9] In any case the effect on the collection efficiency is expected to be even smaller than on the flowfield itself. However the impact distribution will be incorrectly predicted near the nose where the predicted local efficiency is near unity. But a prediction of the local efficiency near the nose can be made by using the method of Ref. 1 for the stagnation region.‡

Figure 8 shows the impact angle for the cone as a function of g_b and f_b. In the use of this graph to obtain, say, the impact angle distribution as a function of body radius, it must be remembered that to each body radius there corresponds a different value of f_b.

Figure 9 shows the impact angle for the power law body with $k = 0.8$. In this case f_b depends, through μ_s, also on the radius of the shock at which the particle enters the shock. Thus, to determine the impact angle along a given body from this graph an iterative procedure should be used similar to the one outlined above for the determination of the efficiency.

The impact velocity is for all computed cases, of course, equal to the freestream velocity within the approximation made.

References

[1] Probstein, R. F. and Fassio, F., "Dusty Hypersonic Flows," *AIAA Journal*, Vol. 8, No. 4, April 1970, pp. 772–779.

[2] Wüst, W., "Hyperschallströmung staubhaltiger Gase bei geringer Dichte," *Zeitschrift für Flugwissenschaften*, Vol. 18, Heft 6, 1970, pp. 185–194.

[3] Sedov, L. I., *Similarity and Dimensional Methods in Mechanics*, Academic Press, New York, 1959.

[4] Carlson, D. J. and Hogland, R. F., "Particle Drag and Heat Transfer in Rocket Nozzles," *AIAA Journal*, Vol. 2, No. 4, April 1964, pp. 1980–1984.

[5] Crowe, C. T., "Drag Coefficient of Particles in a Rocket Nozzle," *AIAA Journal*, Vol. 5, No. 5, May 1967, pp. 1021–1022.

[6] Zarin, N. A., "Measurement of Non-Continuum and Turbulence Effects on Subsonic Sphere Drag," CR-1585, June 1970, NASA.

[7] Schaff, S. A. and Chambre, P. L., "Flow of Rarified Gases," *High Speed Aerodynamics and Jet Propulsion*, Vol. III, edited by H. E. Emmons, Princeton University Press, Princeton, N.J., 1958, pp. 687–739.

[8] Shapiro, A. H., *The Dynamics and Thermodynamics of Compressible Fluid Flow*, Vol. II, Ronald Press, New York, 1954.

[9] Hayes, W. D. and Probstein, R. F., *Hypersonic Flow Theory*, 2nd ed. Vol. 1, Academic Press, New York, 1966.

[10] Chernyi, G. G., "Integral Methods for the Calculation of Gas Flows with Strong Shock Waves," *Prikladnaya Matematika i Mekhanika*, Vol. 25, 1961, pp. 101–107.

[11] Soo, S. L., *Fluid Dynamics of Multiphase Systems*, Blaisdell, Waltham, Mass., 1967.

[12] Waldman, G. D. and Reinecke, W. G., "Particle Trajectories, Heating, and Breakup in Hypersonic Shock Layers," *AIAA Journal*, Vol. 9, No. 6, June 1971, pp. 1040–1048.

‡ See Ref. 12 for objections to this method.